SCALING, MULTIPLICITY DISTRIBUTIONS AND CONSERVATION OF ISOSPIN IN AN UNCORRELATED JET MODEL

By Th. W. Ruijgrok and D. W. Schlitt*

Institute for Theoretical Physics, University of Utrecht**

(Presented by Th. W. Ruijgrok at the XIII Cracow School of Theoretical Physics, Zakopane, June 1–12, 1973)

A simple model for uncorrelated meson production in p-p collisions is extended to include exact conservation of isospin. The correlations between charged particles are so strongly enhanced that the width of the charged particle distribution becomes proportional to the average charged particle multiplicity. For high energies the multiplicity distribution has an energy independent scaling behavior. In the limit of infinite energy this scaling is of the type predicted by Koba, Nielsen and Olesen. The scaling function is singular at a certain value of $N_c/\bar{N}_c$ and beyond this point it vanishes exactly. For large, but not infinite, values of $\bar{N}_c$ the maximum in the topological cross-sections occurs for $N_c/\bar{N}_c$ near this singular point. The value of the maximum cross-section behaves like $\bar{N}_c^{-\frac{3}{4}}\,\sigma_{\text{inel}}$. The model is compared with the results of recent experiments.

1. Introduction and summary

Czyżewski and Rybicki [1] were the first to point out that the prong-number distribution in inelastic πp and pp collisions has a dispersion $D = \sqrt{(N_c - \bar{N}_c)^2}$ which increases linearly with the average charge multiplicity $\bar{N}_c$. Later this was confirmed by Wróblewski [2], who showed that the pp data in the region from 4 to 70 GeV/c are well described by the linear function

$$D = \alpha \bar{N}_c - \beta, \tag{1}$$

where the coefficients α and β are equal within errors, *i. e.*

$$\alpha = \beta = 0.585 \tag{2}$$

with an estimated error of about 0.01. Also for the recently measured energies of 102, 205, and 303 GeV/c formula (1) is very well satisfied as can be seen in Table I.

* Permanent address: Department of Physics, University of Nebraska, Lincoln, Nebraska 68508, USA.

** Address: Inst. voor Theor. Fysica, Rijksuniversiteit, Maliesingel 23, Utrecht, Netherlands.

Another observation first made by Czyżewski and Rybicki [1] is that the prong-number distribution $P(N_c, s)$, probably has a scaling property for the cm energy $\sqrt{s}$ going to infinity. In the language of Koba, Nielsen and Olesen [6] this can be expressed by saying that with increasing s the function

$$\psi(z, s) = \bar{N}_c P(N_c, s), \; z = N_c/\bar{N}_c,$$

tends to a non-trivial function $\psi(z)$. This we will call KNO-scalling. In Ref. [6] it was argued that this follows from Feynman-scaling. The reverse is, however, not necessarily true as we will demonstrate by example in the present paper. Later work [7] seems to confirm this KNO scaling.

TABLE I

Comparison of recent experimental results for $\bar{N}_c$ and D_c with the relation in Eq. (1)

P_{lab}	Ref.	$\bar{N}_c$(exp)	D_c(exp)	D_c(Eq. (1))
102	[4]	6.34 ± 0.14	3.19 ± 0.08	3.12
205	[4]	7.65 ± 0.17	3.88 ± 0.01	3.89
303	[5]	8.86 ± 0.16	4.38 ± 0.11	4.60

It is interesting to find out whether the two phenomena — the linear relation between D and $\bar{N}_c$, and KNO scaling — are manifestations of specific hadronic interactions, or whether they can be understood on the basis of very general properties such as isospin conservation.

In the two-component picture of particle production [8] there is an energy independent (diffractive) contribution to the topological cross-sections as well as an energy dependent part due to pionization. This picture leads easily [8] to $D \sim \bar{N}_c$, or what ammounts to the same thing, to positive correlations in diffractive collisions. For $\bar{p}p$ annihilation no such positive correlations should occur, and they have indeed not yet been found. At ISR energies it will be possible to verify other predictions of the two-component picture [9]. Whether or not for high energies the diffractive process will survive as a cause for positive correlations, it will always be necessary to include the conservation laws as possible sources of correlations. For this reason it is of importance to know the effects of the conservation laws in their purest form. In this spirit the uncorrelated jet model has been used [10] to study the effect of energy and momentum conservation. For high energies no strong correlations were found.

One of the most recent papers on the consequences of isospin conservation was written by Dadič, Martinis and Pisk [11], who also review earlier work on the subject. These authors come to the conclusion that isospin conservation alone gives strong positive correlations. However, the values of α and β found do not agree with those of Eq. (2). The same result was obtained by one of us [12] in a simple unitary model for inelastic $\pi^+ p$ scattering.

In the present paper we construct and discuss a simple model with (1) uncorrelated particle production, and (2) exact (not statistical) conservation of isospin.

The first objective is usually met by taking as the final state

$$|\psi\rangle = e^{-\frac{\lambda}{2}} e^{ga^*}|0\rangle = e^{-\frac{\lambda}{2}} \sum_n \frac{g^n}{\sqrt{n!}} |n\rangle, \tag{3}$$

where $\lambda = |g|^2$. This state gives a Poisson distribution for the multiplicity of the chargeless mesons; momentum dependence is disregarded. In order to incorporate the isospin of the pions we modify the pionic state (3) in a simple way so that it has total isospin I and third component m as follows

$$|lm\rangle = (4\pi f_l(\lambda))^{-\frac{1}{2}} \int d\vec{\tau} Y_{lm}(\vec{\tau}) e^{g\vec{\tau}\cdot\vec{a}^*}|0\rangle, \tag{4}$$

where a $\pi^{\pm}$ and π^0 are created by $a_{\pm}^* = \frac{1}{\sqrt{2}}(a_1^* \pm i a_2^*)$ and a_3^* respectively. It is left to the reader to verify that this state is indeed an eigenstate of I^2 and I_3 with eigenvalues $I(I+1)$ and m and that the normalization constant is

$$f_l(\lambda) = \sqrt{\frac{\pi}{2\lambda}} I_{l+\frac{1}{2}}(\lambda). \tag{5}$$

The function $f_l(\lambda)$ is a modified spherical Bessel function of the first kind [13]. The integration region in (4) is the surface of the unit sphere. If $\frac{1}{2}\vec{\tau}$ is the isospin of a classical nucleon then $|lm\rangle$ can be interpreted as the (l, m)-multipole of the meson field radiated by that nucleon when performing a random motion in isospin space. Irrespective of this interpretation, we will consider the states (4) as the generalization of the uncorrelated state (3). We will use them to construct final states with the same I^2 and I_3 as the initial state. The final state after an inelastic p-p collision is therefore

$$\begin{aligned} |pp\rangle = A(pp)|00\rangle + B\left[\frac{1}{\sqrt{2}}(pp)|10\rangle - \frac{1}{2}(pn+np)|11\rangle\right] + \\ + C\left[\frac{1}{\sqrt{10}}(pp)|20\rangle - \sqrt{\frac{3}{20}}(pn+np)|21\rangle + \sqrt{\frac{3}{5}}(nn)|22\rangle\right] + \\ + \frac{D}{\sqrt{2}}(pn-np)|11\rangle, \end{aligned} \tag{6}$$

where the normalization condition requires

$$|A|^2 + |B|^2 + |C|^2 + |D|^2 = 1. \tag{7}$$

In the term with coefficient D the two nucleons have isospin zero, in the other terms they have $I = 1$. In the same way the final state of a π^-p collision is

$$\begin{aligned} |\pi^- p\rangle = A'n|00\rangle + B'\left[\frac{1}{\sqrt{3}} n|10\rangle - \sqrt{\frac{2}{3}} p|1-1\rangle\right] + \\ + C'\left[\sqrt{\frac{2}{3}} n|10\rangle + \frac{1}{\sqrt{3}} p|1-1\rangle\right] + D'\left[\sqrt{\frac{2}{5}} n|20\rangle - \sqrt{\frac{3}{5}} p|2-1\rangle\right] \end{aligned} \tag{8}$$

with again

$$|A'|^2+|B'|^2+|C'|^2+|D'|^2 = 1. \tag{9}$$

The A' and B' terms have $I = \frac{1}{2}$ and the C' and D' terms have $I = 3/2$. A leading π^- in the final state could be included by adding a term $pa_-^*|0\,0\rangle$. Although this state is already present in the B' and C' terms, it gets an extra weight in this way. For π^+p we take for the final state

$$|\pi^+ p\rangle = Xp|11\rangle + Y[\sqrt{\tfrac{4}{5}}\, n|22\rangle - \sqrt{\tfrac{1}{5}}\, p|21\rangle] \tag{10}$$

with

$$|X|^2+|Y|^2 = 1. \tag{11}$$

Also here a leading π^+ could be described by adding a term $pa_+^*|0\,0\rangle$. The annihilation part of the final state in a $\bar{\text{p}}$-p collision becomes

$$|\bar{p}p\rangle = X'|00\rangle + Y'|10\rangle \tag{12}$$

with

$$|X'|^2+|Y'|^2 = 1. \tag{13}$$

For each of the above processes it is now possible to calculate any multiplicity distribution, branching ratio, or correlation function. A detailed discussion of the results, including fits to the experimental data, will be given in Section 3. For the present, however, we just list the conclusions.

1. The total number of pions, $n = n_+ + n_- + n_0$, has a Poisson-like distribution in the sense that its width increases like $\sqrt{\bar{n}}$. This behaviour is typical for any model with uncorrelated particle emission.

2. The charged particle distribution has a width which increases like $\bar{N}_c$.

3. There are strong positive correlations for pairs of like pions and for pairs of charged pions.

4. There are equally strong negative correlations between a neutral and a charged pion [14].

5. The charged particle distribution shows KNO-scaling in the infinite energy limit.

6. The two-variable distribution $P(n_+, n_+)$ does not scale.

7. The KNO-scaling function for charged particles becomes infinite at a certain finite value z_0 of $z = N_c/\bar{N}_c$. For $z > z_0$ it is equal to zero.

8. For N_c close to $z_0\,\bar{N}_c$ the charged prong topological cross-sections should satisfy a new scaling law. This scaling law also predicts that for high energies the maximum cross-section should occur for N_c equal to $\bar{\bar{N}}_c = z_0\bar{N}_c - \kappa\sqrt{\bar{N}_c}$, where κ is a positive number of order one. The value of this maximum cross-section is predicted to vary like $\bar{N}_c^{-\frac{3}{4}}\,\sigma_{\text{inel}}$.

9. If the energy is $\sqrt{s}$ and the observed prong number is N_c, the average number of neutrals can be considered as a function of s and z. For high energies it turns out to depend on z only and to vanish for $z > z_0$.

2. Detailed discussion of the model

In order to find the distributions functions for the states of Eqs (6), (8), (10) and (12) we must calculate the matrix elements

$$A_l^m(n, n_0) = \langle n_+ n_- n_0 | lm \rangle, \tag{14}$$

where $n = n_+ + n_- + n_0$ and $m = n_+ - n_-$. It is easy to show that

$$A_l^m(n, n_0) = \frac{g^n}{\sqrt{4\pi f_l(\lambda) n_+ ! n_- ! n_0 !}} \int d\vec{\tau} \tau_0^{n_0} \tau_+^{n_+} \tau_-^{n_+} Y_{lm}(\vec{\tau}) \tag{15}$$

with $\tau_0 = \cos\theta$ and $\tau_\pm = \frac{1}{\sqrt{2}}(\tau_1 \pm i\tau_2) = \frac{1}{\sqrt{2}} \sin\theta\, e^{\pm i\Phi}$. From this expression we see that $A_l^m(n, n_0)$ is zero for $n+l$ odd. Since the integral in (15) is just a product of $n+1$ spherical harmonics it is possible to give a closed expression for it [15]. Instead of doing this, we just list the $A_l^m(n, n_0)$ in the Appendix for $l = 0$, 1 and 2.

Let us next consider a final state of the form

$$|\psi\rangle = \sum_{lm} C_{lm} B(l, m) | lm \rangle,$$

where $B(l, m)$ is the baryonic part containing 0, 1, or 2 nucleons. The probability of observing a baryon-meson state $B|n_+ n_- n_0\rangle$ is

$$P(B; n_+ n_- n_0) = |\sum_{lm} C_{lm}(B, B(l, m)) A_l^m(n, n_0)|^2. \tag{16}$$

The only λ dependence is in the A_l^m, the other parameters of the model occur in the C_{lm}. From Eq. (16) we can calculate all the required distributions, averages and branching ratios.

Detailed results for the p-p case will be discussed in Section 3. To illustrate the general properties of the model we will conclude this section with a discussion of the simple case of pp → pp + pions without charge exchange, *i. e.*

$$|\psi\rangle = (\mathrm{pp})|0\,0\rangle. \tag{17}$$

In this case the probability of finding n pions, among which there are n_0 neutral pions is

$$P_\lambda(n, n_0) = \frac{\lambda^n}{f_0(\lambda)} \frac{1}{n_0!} \left[\frac{(n_0-1)!!}{(n+1)!!}\right]^2, \tag{18}$$

where $f_0(\lambda) = \lambda^{-1} \sinh\lambda$. The probability is zero unless both n and n_0 are even. Summing Eq. (18) over all even $n_0 \leqslant n$ gives the distribution of the total number of pions:

$$P(n) = \frac{1}{\sinh\lambda} \cdot \frac{\lambda^{2j+1}}{(2j+1)!}, \tag{19}$$

where $n = 2j$. This is a Poisson-like distribution with an average number

$$\bar{n} = \frac{\lambda}{\mathrm{tgh}\,\lambda} - 1 \tag{20}$$

and a dispersion

$$D^2 = \overline{(n-\bar{n})^2} = \frac{\lambda}{\operatorname{tgh}\lambda} - \left(\frac{\lambda}{\sinh\lambda}\right)^2. \tag{21}$$

The two particle correlation is

$$f_2 = \overline{n(n-1)} - \bar{n}^2 = D^2 - \bar{n} = 1 - \left(\frac{\lambda}{\sinh\lambda}\right)^2. \tag{22}$$

For λ, which in this model plays the role of the energy parameter, going to infinity, we find the following asymptotic expressions:

$$\bar{n} \simeq \lambda - 1 + \ldots, \quad D^2 \simeq \lambda + \ldots, \quad f_2 \simeq 1 + \ldots, \tag{23}$$

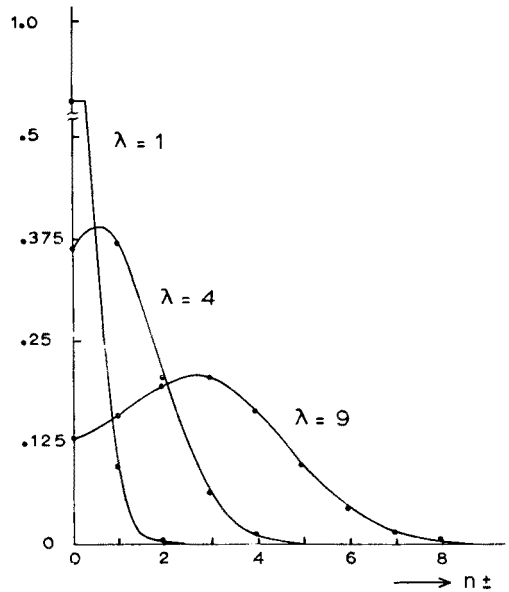

Fig. 1. The probability distribution for $\pi^{\pm}$ as predicted by the model for various values of λ in the case of no charge exchange

where the remaining terms are all of order $\exp(-2\lambda)$. From Eq. (18) we also find that the average multiplicity of the charged and neutral pions is $\bar{n}_+ = \bar{n}_- = \bar{n}_0 = \frac{1}{3}\bar{n}$. Adding in the two protons gives for the average charged particle multiplicity in the limit of large λ:

$$\bar{N}_c \simeq \tfrac{2}{3}\lambda + \tfrac{4}{3} + \ldots. \tag{24}$$

Although the average numbers of π^+, π^- and π^0 are equal, their distributions are quite different as in shown in Fig. 1 and 2. The charged pions have a distribution with a maximum which for increasing energy shifts to higher multiplicities. The distribution of neutral pions has its maximum always at $n_0 = 0$. The reason for this peculiar difference is that

for fixed number of charged mesons the neutrals form a one-dimensional subspace while for fixed number of neutral mesons the charged mesons form a two-dimensional subspace. One can also compute the two particle correlations:

$$\begin{aligned} f_{2\pm} &= \overline{n_\pm(n_\pm-1)}-\bar{n}_\pm^2, \\ f_{20} &= \overline{n_0(n_0-1)}-\bar{n}_0^2, \\ f_{+-} &= \overline{n_+n_-}-\bar{n}_+\bar{n}_-, \\ f_{\pm 0} &= \overline{n_\pm n_0}-\bar{n}_\pm\bar{n}_0. \end{aligned} \tag{25}$$

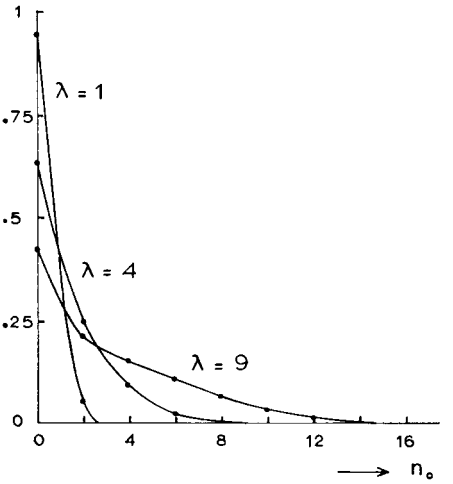

Fig. 2. The probability distribution for π^0 as predicted by the model for various values of λ in the case of no charge exchange

The charged meson correlation

$$f_{2c} = n_c(n_c-1)-\bar{n}_c^2 \text{ with } n_c = n_+ + n_-$$

and the total two particle correlation f_2 (Fig. 2) are related to the above as follows:

$$f_{2c} = f_{2+}+f_{2-}+2f_{+-} \tag{26}$$

and

$$f_2 = f_{2c}+f_{20}+2(f_{+0}+f_{-0}). \tag{27}$$

For high energies ($\lambda \to \infty$) we find the following asymptotic expressions:

$$f_{2\pm} \simeq \frac{1}{45}\lambda^2 - \frac{8}{45}\lambda + \ldots,$$

$$f_{20} \simeq \frac{4}{45}\lambda^2 - \frac{2}{45}\lambda + \ldots,$$

$$f_{+-} \simeq \frac{1}{45}\lambda^2 + \frac{7}{45}\lambda + \ldots,$$

$$f_{\pm 0} \simeq -\frac{2}{45}\lambda^2 + \frac{1}{45}\lambda + \ldots, \tag{28}$$

where the remaining terms are $O(1)$. Due to the strong positive correlations between charged particles we find that f_{2c} is also large and positive:

$$f_{2c} \simeq \frac{4}{45}\lambda^2 - \frac{2}{45}\lambda + \ldots \tag{29}$$

i. e., the same as f_{20}. The charged-neutral correlation is negative and cancels the positive correlation so that $f_2 \simeq O(1)$, as was already found in Eq. (23). From Eq. (29) we can derive the dispersion of the charged pion distribution with the result

$$D_c \simeq \frac{1}{\sqrt{5}}\bar{n}_c + \frac{3}{\sqrt{5}} + \ldots. \tag{30}$$

The coefficient $1/\sqrt{5} = 0.447$ is the same as found by Dadič *et al.* [11]. For $\pi^{\pm}$p this coefficient is practically equal to the experimental value of 0.44 quoted by Wróblewski [2]. It is, however, quite different from the value 0.585 ± 0.01 for p-p scattering. In our model the coefficient will be changed by adjusting the values of the parameters in Eq. (6). The results of this adjustment will be discussed in Section 3 where the effects of the nucleons will also be included.

From Eq. (30) it is clear that the distribution of the number of charged pions is much broader than a Poisson-distribution. Summing Eq. (18) over the neutrals gives for even n_c

$$P_\lambda(n_c) = \frac{\lambda^{n_c}}{f_0(\lambda)} \sum_{n_0=0,2,4,\ldots} \frac{\lambda^{n_0}}{n_0!} \left[\frac{(n_0-1)!!}{(n_c+n_0+1)!!}\right]^2. \tag{31}$$

Next let us examine the large λ behaviour of this distribution. In particular we are interested in the scaling properties of the distribution. First we will give a rather general argument that it scales in the sense of KNO [6], *i. e.*, that there exists a non-trivial function $\psi(u)$ defined by

$$\psi(u) = \lim \lambda P_\lambda(n_c) \tag{32}$$

where λ and n_c both go to infinity, but in such a way that $u = n_c/\lambda$ remains constant. The KNO variable $z = N_c/\bar{N}_c$ is simply related to this u. The argument proceeds by examining the moments $d_k = \overline{(n_c - \bar{n}_c)^k}$, where the averages are defined with the distribution $P_\lambda(n_c)$. We have shown (Eq. (23) and (30)) that $\bar{n}_c = O(\lambda)$ and $d_2 = O(\lambda^2)$. From the assumption of uncorrelated production it follows that d_k is at most $O(\lambda^k)$. This is a consequence of the fact that in the state $|lm\rangle$ the amplitude for finding k pions occurs with a coefficient proportional to g^k. In principle it is not exclud d that cancellations occur and that d_k is actually of lower order. We will now prove by induction that this is not the case for

even k. Suppose $d_{2k} = O(\lambda^{2k})$. In the Schwartz inequality

$$|\overline{AB}|^2 \leqslant \overline{A^2} \cdot \overline{B^2}$$

take $A_n = (n-\bar{n})^{k+1}$ and $B_n = (n-\bar{n})^{k-1}$. This gives

$$|d_{2k}|^2 \leqslant d_{2k+2} \cdot d_{2k-2}$$

or

$$d_{2k+2} \geqslant \frac{|d_{2k}|^2}{d_{2k-2}} = O(\lambda^{2k+2}).$$

We know that d_{2k+2} is at most $O(\lambda^{2k+2})$ so that also $d_{2k+2} = O(\lambda^{2k+2})$ which proves that

$$d_{2k} = O(\lambda^{2k}) \quad \text{for all } k = 1, 2, \ldots . \tag{33}$$

Consider next the even moments of $\psi(u)$:

$$a_{2k} = \int_0^\infty \psi(u)\,(u-\bar{u})^{2k} du \Big/ \int_0^\infty \psi(u) du,$$

where

$$\int_0^\infty \psi(u) du = \lim \frac{2}{\lambda} \sum_{n_c} \lambda P_\lambda(n_c) = 2 \tag{34}$$

and

$$\bar{u} = \frac{1}{2} \int_0^\infty u\psi(u) du = \frac{1}{2} \lim \frac{2}{\lambda} \sum_{n_c} \frac{n_c}{\lambda} \cdot \lambda P_\lambda(n_c) = \lim \frac{\bar{n}_c}{\lambda}. \tag{35}$$

The even moments then become

$$a_{2k} = \frac{1}{2} \sum_{n_c} \frac{2}{\lambda} \cdot \lambda P_\lambda(n_c) \left(\frac{n_c}{\lambda} - \frac{\bar{n}_c}{\lambda} \right)^{2k} = \frac{d_{2k}}{\lambda^{2k}}. \tag{36}$$

Because of (33) it now follows that all even moments of $\psi(u)$ exist and are finite. Some of the odd moments may be zero, but are certainly not infinite. Although the moment problem does not always have a unique solution (*cf.* the discussion in Ref. [6] on this point) the argument given above is a strong indication that KNO-scaling occurs as soon as there is uncorrelated particle emission and $D_c \sim \bar{N}_c$. In the present case we have shown the KNO-scaling by actual calculation of the function $\psi(u)$.

Koba, Nielsen and Olesen derived their scaling law from Feynman-scaling. This also led to scaling of $P_\lambda(n, n_0)$ in the sense that the limit of $\lambda^2 P_\lambda(n, n_0)$ for $\lambda \to \infty$, $n_c \to \infty$ and $n_0 \to \infty$, but with fixed $u_1 = n_c/\lambda$ and $u_2 = n_0/\lambda$, exists and is a function $\psi(u_1, u_2)$ of

u_1 and u_2 alone. In the present case we find that

$$\lambda^2 P_\lambda(n, n_0) \sim \lambda^{\frac{1}{2}} e^{-\lambda g(u_1, u_2)} \tag{37}$$

with $g(u_1, u_2) = 1+u_2+(u_1+u_2)\ln(u_1+u_2)$. Since $g(u_1, u_2) > 0$ for all positive u_1 and u_2, the function in Eq. (37) goes to zero as $\lambda \to \infty$. These two results show that Feynman-scaling is not a necessary condition for KNO-scaling.

Next we give a direct calculation of the function $\psi(u)$ of Eq. (32). The result can be obtained in a number of ways. The one presented here is perhaps the most transparent. Using well known properties of the Γ-function [16] we obtain

$$\lambda P_\lambda(n_c) \simeq 2e^{-\frac{2l}{u}} \sum_{k=1}^{\infty} \left(\frac{2l}{u}\right)^{2k+2l+2} \frac{\sqrt{1+\dfrac{l+1}{k}}}{(2k+2l+2)!}, \tag{38}$$

where $n_0 = 2k$, $n_c = 2l = \lambda u$, and where we have neglected the term in the original expression (31) with $n_0 = 0$. The expression (38) can further be approximated by

$$\lambda P_\lambda(n_c) \simeq \sum_{n_0>0} W(n_0) \sqrt{1+\frac{n_c}{n_0}}, \tag{39}$$

where

$$W(n_0) = e^{-\frac{n_c}{u}} \frac{\left(\dfrac{n_c}{u}\right)^{n_0+n_c}}{(n_0+n_c)!}, \qquad n_0 = -n_c, -n_c+1, \ldots \tag{40}$$

is a normalized Poisson distribution with average

$$\bar{n}_0 = \left(\frac{1}{u} - 1\right) n_c \tag{41}$$

and dispersion

$$D = \sqrt{\overline{(n_0-\bar{n}_0)^2}} = \sqrt{\frac{n_c}{u}}. \tag{42}$$

We now distinguish between the following three cases:

a. $\bar{n}_0 < 0$ and $|\bar{n}_0| \gg D$ or $u > 1$ and $u-1 \gg D^{-1}$,
b. $\bar{n}_0 > 0$ and $\bar{n}_0 \gg D$ or $u < 1$ and $1-u \gg D^{-1}$,
c. $|\bar{n}_0| \lesssim D$ or $|1-u| \lesssim \dfrac{1}{\sqrt{n_c}}$.

In case a the peak of the distribution function $W(n_0)$ falls completely outside the range of the summation. We therefore find that

$$\psi(u) = 0 \text{ for } u-1 \gg D^{-1}. \tag{43}$$

In case b the peak of $W(n_0)$ falls completely inside the region of summation. Since $\sqrt{1+n_c/n_0}$ varies but slowly over the width D of the peak, we find

$$\lambda P_\lambda(n_c) \simeq \sqrt{1+\frac{n_c}{\bar{n}_0}} \tag{44}$$

or

$$\psi(u) = \frac{1}{\sqrt{1-u}} \quad \text{for} \quad 1-u \gg D^{-1}. \tag{45}$$

In the limit that λ and n_c actually become infinite we see that $\psi(u)$ has a singular point at $u = 1$.

For λ and n_c large, but not infinite, there is an intermediate region, case c. In this case a finite fraction of the peak falls inside the region of summation. We now approximate $W(n_0)$ by a Gaussian distribution with the same $\bar{n}_0$ and D,

$$W(n_0) \approx \sqrt{\frac{u}{2\pi n_c}}\, e^{-\frac{u}{2n_c}(n_0-\bar{n}_0)^2}, \quad u \approx 1 \tag{46}$$

and replace the summation over n_0 by an integration over $y = n_0/\sqrt{2n_c}$. This gives

$$\lambda P_\lambda(n_c) \simeq \left(\frac{n_c}{2}\right)^{\frac{1}{4}} G(\bar{y}) \tag{47}$$

with

$$G(\bar{y}) = \frac{1}{\sqrt{\pi}} \int_0^\infty \frac{e^{-(y-\bar{y})^2}}{\sqrt{y}}\, dy$$

and

$$\bar{y} = \frac{\bar{n}_0}{\sqrt{2n_c}} = (1-u)\sqrt{\frac{n_c}{2}}. \tag{48}$$

The function $G(\bar{y})$ provides a smooth transition between the two cases a and b. For $\bar{y}$ large and negative, which corresponds to $u > 1$ it approaches zero and we have case a. If $\bar{y} \gg 1$, corresponding to $u < 1$ we have

$$G(\bar{y}) \simeq \frac{1}{\sqrt{\bar{y}}}$$

and

$$\lambda P_\lambda(n_c) \simeq \frac{1}{\sqrt{1-u}}.$$

This is just the result for case b.

The function $G(\bar{y})$ is plotted in Fig. 3. It has the property that it has a maximum value at $\bar{y} = y_0 = 0.544$ with value $G_0 = 1.2235$. This means that for large values of $\bar{n}_c$ the cross-section $\sigma_{n_c}(\bar{n}_c)$ has a maximum for

$$n_c \simeq \tfrac{3}{2}\bar{n}_c - y_0\sqrt{3\bar{n}_c}\,. \tag{49}$$

The value of this maximum is

$$S(\bar{n}_c) \equiv \operatorname*{Max}_{n_c} \sigma_{n_c}(\bar{n}_c) \simeq \frac{1}{2}\left(\frac{4}{3\bar{n}_c}\right)^{3/4} G_0\sigma_{\text{inel}}(\bar{n}_c) = 0.759\,\bar{n}_c^{-3/4}\sigma_{\text{inel}}(\bar{n}_c). \tag{50}$$

The numerical constant in this equation will change with the parameters of the model but the $\bar{n}_c$ dependence remains the same. Since σ_{inel} seems to increase like $\bar{n}_c^2$ [17], it follows that $S(\bar{n}_c)$ increases like $\bar{n}_c^{5/4}$.

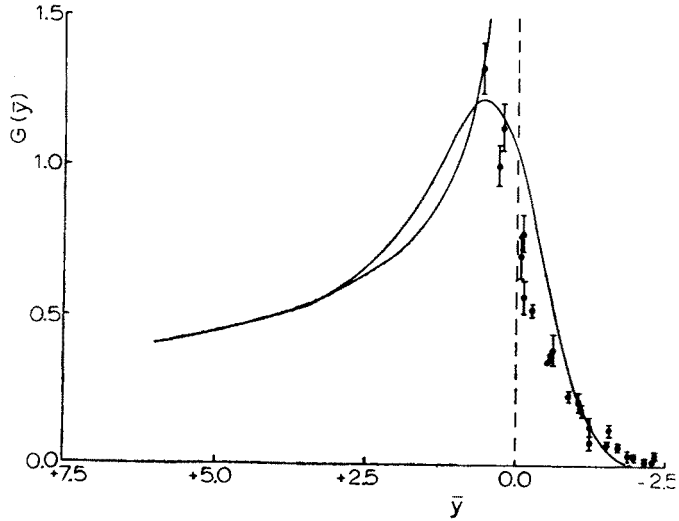

Fig. 3. The scaling function $G(\bar{y})$. For comparison the limiting form with its singularity at $\bar{y} = 0$ is shown. Also plotted are the experimental values as described in Section 3 for $N_c \geqslant 10$ and $P_{\text{lab}} = 50$, 69, 102, 205, and 303 GeV/c

The function $G(\bar{y})$ can be looked upon as a scaling function in a new scaling law implied by Eq. (47). In the next Section we will compare both this new scaling and the KNO-scaling predicted by this model with the experimental data.

In the same way as we calculated the scaling function $\psi(u)$, we can also determine the average number of neutral pions for a given number of charged pions. In the limit $\lambda \to \infty$, $n_c \to \infty$, but $u = n_c/\lambda$ fixed we again find scaling and the limiting behaviour is

$$\bar{n}_0(n_c) \to \begin{cases} \sqrt{1-u} & \text{for } u < 1, \\ 0 & \text{for } u > 1. \end{cases} \tag{51}$$

This formula is another manifestation of the strong correlation between the neutral and charged pions in this model. To obtain the quantity usually reported in experimental papers this value of $\bar{n}_0(n_c)$ should be divided by $\sigma_{n_c}/\sigma_{\text{inel}}$.

3. Comparison with experimental results

The properties of this model as described in the preceeding Section give some hope that the model will be in good agreement with experimental observations. Any precise comparisons require that values be given for the various parameters which enter into equation (6). The method chosen was to determine the constants by fitting the model to the experimental topological cross-sections [3, 4, 5, 18, 19, 20, 21]. The strategy which was eventually used was the outcome of an extensive investigation of the possibilities.

The parameters which must be determined are λ, $|A|^2 = AA$, $|B|^2 = BB$, $|C|^2 = CC$, $|D|^2 = DD$ and the phase between the complex numbers A and C, which enters as $\cos \varphi_{AC} = RE$. The fits to the data were made by minimizing χ^2 using the Rostock method of minimization.

By examining the data a single energy at a time it was observed that most of the energy dependence would be represented by letting λ depend linearly on $\ln P_{\text{lab}}$. The other parameters could then be taken as energy independent. It was also observed that the low multiplicity cross-sections were fit badly by the model. This is not unexpected in light of the current evidence that the low multiplicity events have a significant diffractive component [8, 9]. In order to include this effect without increasing the number of free parameters unduly we introduced 3 energy independent diffractive components $\sigma_D(2)$, $\sigma_D(4)$ and $\sigma_D(6)$ in the 2, 4 and 6 prong cross-sections respectively. A final determination of the parameters was made using the parameters a and b in

$$\lambda = a + b \log_{10} P_{\text{lab}}, \tag{52}$$

the four parameters, AA, BB, CC and DD which, in fact, give only three free parameters because of the normalization condition (7); the phase RE and finally the three diffractive cross-sections. Thus there are a total of nine parameters to be determined.

Perhaps as much was learned about the properties of the model in the process of choosing the parameters as can be learned from the final choice of parameters. Provided λ was chosen properly by appropriate choice of a and b the other parameters of the model could be chosen more or less freely without drastic changes in the fit to the data; part of the change in the multiplicity distribution being compensated by changes in the diffractive component. The diffractive contribution to the 2 prong cross-section was always small and the total diffractive contribution does not vary significantly. A model such as this with independent particle production is expected to be best at high energies where threshold effects and resonance production are unimportant. This was found to be the case but not dramatically so. Fits made to the seven energies, 19 [18], 28.5 [19], 50 [21], 69 [21], 102 [3], 205 [4] and 303 [5] GeV/c typically gave χ^2 of $\sim$ 190 for 63 data points. Fits to the highest 5 energies were somewhat better giving χ^2 of $\sim$ 90 for 50 data points. Fits using only the highest three energies were best and will be used for the remaining discussion.

As has been noted by others [9], the two prong cross-section at 303 GeV/c seems to be too low in comparison with those at lower energies. We have used the published value for the total two prong cross-section but have used an elastic cross-section of 6.8 mb as found in recent ISR experiments [17] at comparable energies, instead of the value of

7.2 mb as used in the paper. Finally, we observed a tendency for the value of DD to be small. This has a simple physical meaning: the $I = 0$ state of the two nucleons is suppressed relative to the $I = 1$ state. We have therefore chosen DD identically zero.

The best fit to the topological cross-sections at the three highest energies gave a χ^2 of 43.8 for 33 data points and 8 free parameters. The values of the parameters were

$$\begin{array}{lll} a = -6.33 & \sigma_D(2) = 0.187 & AA = 0.178 \\ b = \ \ 7.39 & \sigma_D(4) = 1.505 & BB = 0.576 \\ & \sigma_D(6) = 1.535 & CC = 0.246 \\ & \overline{\qquad\qquad\qquad} & DD = 0.0 \\ & \sigma_D \ \ = 3.23 \text{ mb} & RE = -0.503 \end{array} \tag{53}$$

In Table II we show a comparison of the experimental values of $\overline{N}_c$ and D_c with those given by the model. Asymptotically we find

$$D_c \simeq 0.58\,(N_c - 3.29). \tag{54}$$

In Fig. 4 the topological cross-sections predicted by the model are plotted for P_{lab} from 15 to 1500 GeV/c. For comparison the experimental points are also plotted. Since the

TABLE II

Comparison of experimental values of $\overline{N}_c$ and D_c with those predicted by the model with the parameters of Eq. (53)

P_{lab}	$\overline{N}_c$(exp)	$\overline{N}_c$(th.)	D_c(exp.)	N_c(th.)
102	6.34 ± 0.14	6.28	3.19 ± 0.08	3.12
205	7.65 ± 0.17	7.60	3.88 ± 0.08	3.84
303	8.77 ± 0.20[a]	8.35	4.35 ± 0.15[a]	4.26

[a] The two prong cross-section has been adjusted as described in the text.

parameters are chosen to optimize the fit at high energies the fit at lower energies is not good. The fit to the low energy data can be improved by a different choice of parameters. In Fig. 5 we show the topological cross-sections at 205 GeV/c as predicted by the model and from experiment. The diffractive contribution is indicated. The break in the curve between $N_c = 6$ and 8 indicates that an 8 prong diffractive component is probably present.

Next we look at the various scaling properties of the model. The presence of a diffractive contribution complicates the situation. In Fig. 6 we show the KNO scaling function predicted by the model along with the experimental data and the curve given by the model for 303 GeV/c. We see that both the experimental data and the model are far from the limiting behaviour that is predicted. In the limit the diffractive component should give a delta-function contribution at $z = 0$. While the major portion of the peak for z less than 1 is the diffractive component we see that it is far from a delta-function. In spite of the clustering of the experimental data in a narrow band we must conclude that we are far from the scaling limit. In Fig. 3 we have plotted the experimental data under the assumption

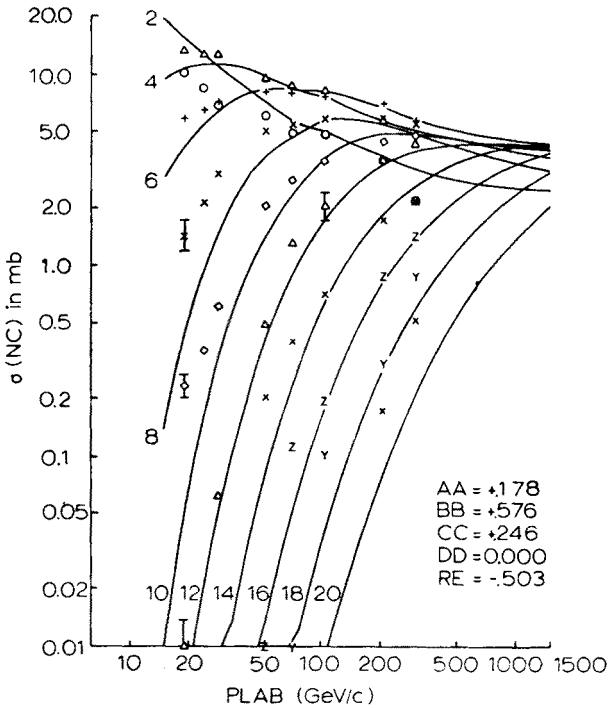

Fig. 4. The charged prong topological cross-sections predicted by the model with the parameters (53). The experimental data of Refs [3, 4, 5, 18, 19, 20, 21] are shown along with some typical error bars

that it scales according to Eq. (47) with $n_c = N_c$. The general form of the scaling relation is in this case

$$\bar{N}_c \frac{\sigma_{N_c}}{\sigma_{\text{nel}}} \simeq \left(\frac{N_c}{2}\right)^{\frac{1}{2}} xQG(\bar{y}), \tag{55}$$

where

$$x = \frac{2}{3} - \frac{R}{15}, \qquad Q = 1 - \frac{R}{4}, \qquad R = 2\sqrt{2}\,(AA \cdot CC)^{\frac{1}{4}}\, RE + BB - CC - 2.DD$$

and

$$\bar{y} = \left(\frac{N_c}{2}\right)^{\frac{1}{2}} \left(1 - \frac{xN_c}{\bar{N}_c}\right).$$

While there is not striking agreement, the data agrees with this scaling better than it does with the KNO limiting curve.

The model makes predictions about various average multiplicities. The average charged particle multiplicity is given as a function of P_{lab} by

$$\bar{N}_c \simeq 2.14 \ln P_{\text{lab}} - 3.54. \tag{56}$$

The average number of neutral pions is related to the average number of negatives by

$$\bar{n}_0 \simeq \bar{n}_- + 0.329.$$

In Fig. 7 we show a comparison of this prediction with the experimental data. In this model the average number of neutrons is independent of λ and therefore of P_{lab}. The value given by the model is 0.657. This corresponds to an average number of protons of 1.34

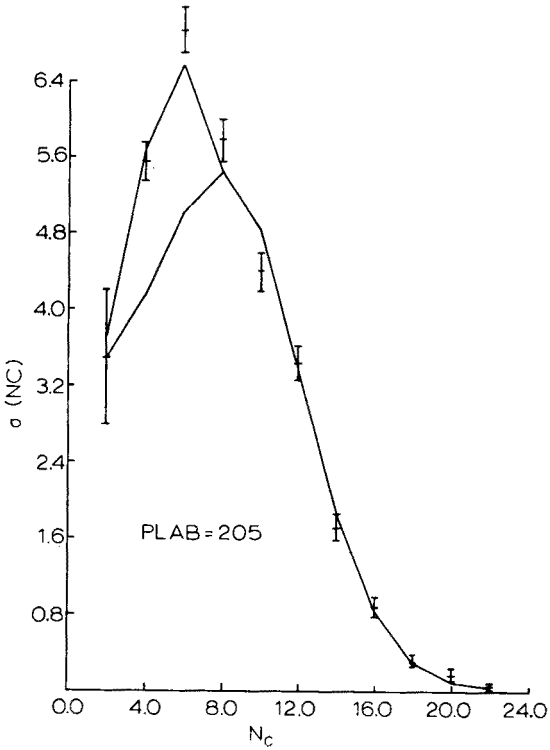

Fig. 5. The charged prong topological cross-sections for $P_{\text{lab}} = 205$ GeV/c. The contribution of the diffractive component is the difference between the two lines

which is in agreement with experimental measurements [22]. In Fig. 8 we show the π^0 multiplicity distribution. We see that in this model the peak in the distribution for low multiplicities comes from the pn and nn final states while the high multiplicity part goes with the pp final state.

Finally we have computed the prediction of the model for the experimentally measured quantity, the average number of π^0 for a fixed number of charged particles. The results are shown in Fig. 9 along with the experimental results [23]. There is a striking disagreement between the model and experiment. The strong peaking for low N_c in the model is related to the strong negative correlations between charged and neutral pions in the model which are required to give a broad charged particle distribution. If we started from a total

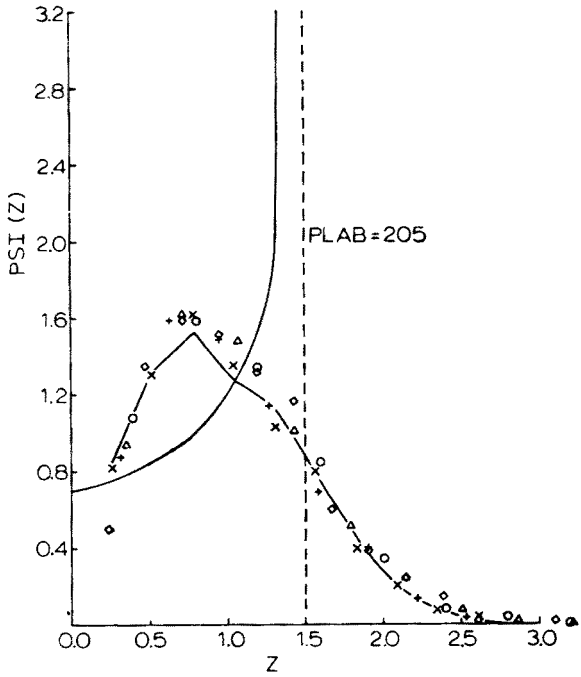

Fig. 6. The KNO scaling function. The curve which is singular at $z = 1.5$ is the infinite energy limit as predicted by the model. The second curve is that given by the model for 303 GeV/c. The experimental points are those from Ref. [7]

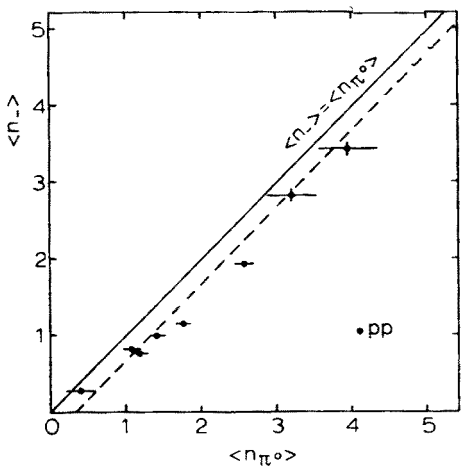

Fig. 7. The relationship between the average number of neutral pions and the average number of negative pions. The line is the high energy relation predicted by the model. This figure was kindly provided by Prof. A. Wróblewski

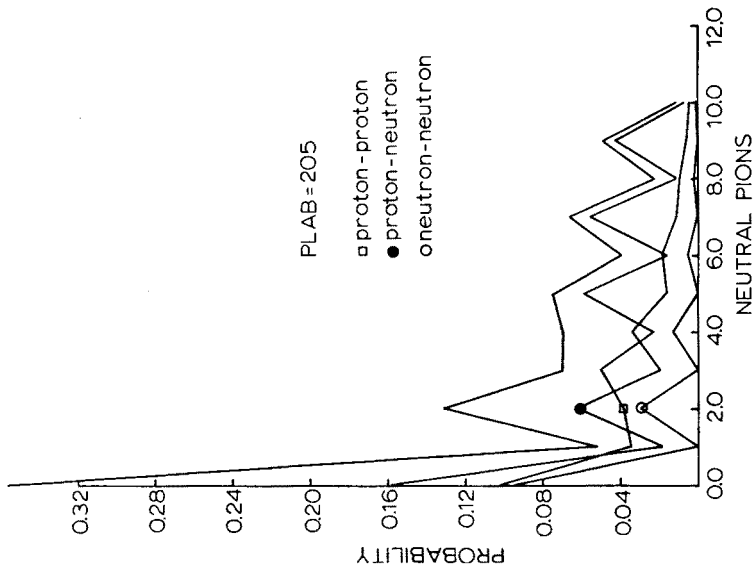

Fig. 8. The probability distribution of neutral pions given by the model with the parameters (53) and $P_{lab} = 205$ GeV/c. The upper line in the total distribution; the other lines show the contributions of the pp, pn and nn final states

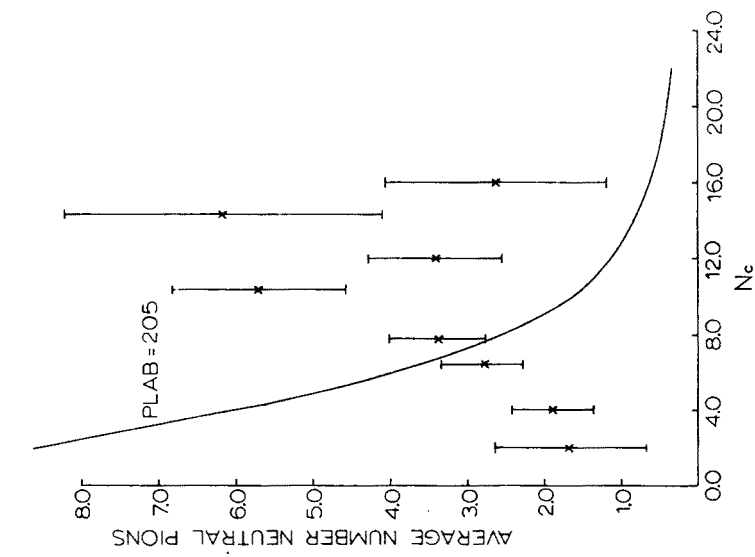

Fig. 9. The average number of neutral pions for a fixed number of charged particles. The curve is the result predicted by the model (excluding the diffractive contribution to π^0 production) at 205 GeV/c. The experimental data are from Ref. [22]

pion distribution which was broader than Poisson, instead of that required by uncorrelated particle emission, it is possible that we would obtain better agreement for this quantity.

It is a great pleasure to thank Professor A. Białas for exciting discussions and correspondence while this paper was written.

APPENDIX

In this Appendix we list the non-vanishing $A_l^m(n, n_0)$ for $l = 0$, 1 and 2. $n+l$ must be even and $m = n_+ - n_-$. For a given l and m these two restrictions determine whether n_0 is even or odd.

$l = 0$, n even

$$A_0^0(n, n_0) = \sqrt{\frac{\lambda^n}{f_0(\lambda)}} \cdot \frac{1}{\sqrt{n_0!}} \cdot \frac{(n_0-1)!!}{(n+1)!!} \quad (n_0 \text{ even})$$

$l = 1$, n odd

$$A_1^0(n, n_0) = \sqrt{\frac{\lambda^n}{f_1(\lambda)}} \cdot \frac{\sqrt{3}}{\sqrt{n_0!}} \cdot \frac{n_0!!}{(n+2)!!} \quad (n_0 \text{ odd})$$

$$A_1^{\pm 1}(n, n_0) = \mp \sqrt{\frac{\lambda^n}{f_1(\lambda)}} \cdot \frac{\sqrt{\frac{3}{2}(n-n_0+1)}}{\sqrt{n_0!}} \cdot \frac{(n_0-1)!!}{(n+2)!!} \quad (n_0 \text{ even})$$

$l = 2$, n even

$$A_2^0(n, n_0) = \sqrt{\frac{\lambda^n}{f_2(\lambda)}} \cdot \frac{\sqrt{5}}{2} \cdot \frac{(3n_0-n)}{\sqrt{n_0!}} \cdot \frac{(n_0-1)!!}{(n+3)!!} \quad (n_0 \text{ even})$$

$$A_2^{\pm 1}(n, n_0) = \mp \sqrt{\frac{\lambda^n}{f_2(\lambda)}} \cdot \frac{\sqrt{30}}{2} \cdot \frac{\sqrt{n-n_0+1}}{\sqrt{n_0!}} \cdot \frac{n_0!!}{(n+3)!!} \quad (n_0 \text{ odd})$$

$$A_2^{\pm 2}(n, n_0) = \sqrt{\frac{\lambda^n}{f_2(\lambda)}} \cdot \frac{\sqrt{30}}{4} \cdot \frac{\sqrt{(n-n_0)(n-n_0+2)}}{\sqrt{n_0!}} \cdot \frac{(n_0-1)!!}{(n+3)!!} \quad (n_0 \text{ even})$$

REFERENCES

[1] O. Czyżewski, K. Rybicki, *Nuclear Phys.*, **B47**, 633 (1972) and earlier work quoted there.

[2] A. Wróblewski, *Remarks on Current Models for Charged Multiplicity Distributions*, Warsaw preprint IFD/72/2.

[3] J. W. Chapman, N. Green, B. P. Roe, A. A. Seidl, D. Sinclair, J. C. Van der Velde, C. M. Bromberg, D. Cohen, T. Ferbel, P. Slattery, S. Stone, B. Werner, *Phys. Rev. Letters*, **29**, 1686 (1972).

[4] G. Charlton, Y. Cho, M. Derrick, R. Engelmann, T. Fields, L, Hyman, K. Jaeger, U. Mehtani, B. Musgrave, Y. Oren, D. Rhines, P. Schreiner, H. Yuta, L. Voyvodic, R. Walker, J. Whitmore, H. B. Crawley, Z. Ming Ma, R. G. Glasser, *Phys. Rev. Letters*, **29**, 515 (1972).

[5] F. T. Dao, D. Gordon, J. Lach, E. Malamud, T. Meyer, R. Poster, W. Slater, *Phys. Rev. Letters*, **29**, 1627 (1972).
[6] Z. Koba, H. B. Nielsen, P. Olesen, *Nuclear Phys.*, **B40**, 317 (1972).
[7] P. Slattery, *Phys. Rev. Letters*, **29**, 1624 (1972); *Phys. Rev.*, **D7**, 2073 (1973).
[8] A. Białas, K. Fiałkowski, K. Zalewski, *Nuclear Phys.*, **B48**, 237 (1972); L. Van Hove, *Phys. Letters*, **43B**, 65 (1973); H. Harari, E. Rabinovici, *Phys. Letters*, **43B**, 49 (1973).
[9] K. Fiałkowski, H. I. Miettinen, *Phys. Letters*, **43B**, 61 (1973).
[10] E. H. de Groot, Th. W. Ruijgrok, *Nuclear Phys.*, **B27**, 45 (1971); S. Sohlo, *Nuclear Phys.*, **B53**, 410 (1973); O. Korosuo, S. Sohlo, *Energy-Momentum Conservation Effects in the Inclusive Two Particle Correlation from 18 GeV/c to ISR Energy*, Research Report No 3/1973, Department of Physics, University of Jyväskylä, Finland, February 1973.
[11] I. Dadič, M. Martinis, K. Pisk, *Nuovo Cimento*, **13A**, 777 (1973).
[12] Th. W. Ruijgrok, *Long Lange Order in an Uncorrelated Jet Model*, Paper 29 submitted to the Third International Colloquium on Multiparticle Reactions, Zakopane, Poland, June 1972.
[13] M. Abramowitz, I. A. Stegun, *Handbook of Mathematical Functions*, Dover Publications Inc., New York 1965.
[14] This is a general property of uncorrelated emission models. For an extensive discussion see D. W. Schlitt and Th. W. Ruijgrok, paper submitted to the *II Aix-en-Provence International Conference on Elementary Particles*, September 1973.
[15] A. P. Yutsis, I. B. Levinson, V. V. Vanagas, *The Theory of Angular Momentum*, Israël Program for Scientific Translations, Jerusalem 1962, p. 30.
[16] Ref. [13] formula 6.1.49, p. 258 and 6.1.18, p. 256.
[17] S. R. Amendolia, G. Bellettini, P. L. Braccini, C. Bradaschia, R. Castaldi, V. Cavasinni, C. Cerri, T. Del Prete, L. Foa, P. Giromini, P. Laurelli, A. Menzione, L. Ristori, G. Sanguinetti, M. Valdata, G. Finocchiaro, P. Grannis, D. Green, R. Mustard, R. Thun, *Phys. Letters*, **44B**, 119 (1973) and to be published.
[18] H. Bøggild, E. Dahl-Jensen, K. H. Hansen, J. Johnstadt, E. Lohse, M. Suk, L. Veje, V. J. Karimaki, K. V. Laurikainen, R. Riipinen, T. Jacobsen, S. O. Sørensen, J. Allan, G. Blomquist, O. Danielsen, G. Ekspong, L. Granstrøm, S. O. Holmgren, S. Nilsson, B. E. Ronne, U. Svedin, M. K. Yamdagni, *Nuclear Phys.*, **B27**, 285 (1971).
[19] W. H. Sims, J. Hanlon, E. O. Salant, R. S. Panvini, R. R. Kinsey, T. W. Morris, L. Von Lindern, *Nuclear Phys.*, **B41**, 317 (1972).
[20] S. Nilsson, F. Breivik, T. Buran, H. Tøfte, *Nuovo Cimento*, **43A**, 716 (1966).
[21] V. V. Ammosov, V. N. Boitsov, P. F. Ermolov, A. B. Fenyuk, P. A. Gorichev, E. P. Kistenev, S. V. Klimenko, B. A. Manyukov, A. M. Moiseev, R. M. Sulyaev, S. M. Tarasevich, A. P. Vorobjev, H. Blumenfeld, J. Derre, P. Granet, M. A. Jabiol, A. Leveque, M. Loret, E. Pauli, Y. Pons, J. Prevost, J. C. Scheuer, M. Boratav, J. Laberrigue, H. K. Nguyen, S. Orenstein, *Phys. Letters*, **42B**, 519 (1972).
[22] M. Antinucci, A. Bertin, P. Capiluppi, M. D'Agostino-Bruno, A. M. Rossi, G. Vannini, G. Giacomelli, A. Bussière, *Lett. Nuovo Cimento*, **6**, 121 (1973).
[23] G. Charlton *et al.*, *Phys. Rev. Letters*, **29**, 1759 (1972).